

REDISCUSSION OF ECLIPSING BINARIES. PAPER V.
THE TRIPLE SYSTEM V455 AURIGAE

By John Southworth

Astrophysics Group, Keele University, Staffordshire, ST5 5BG, UK

V455 Aur is a detached eclipsing binary containing two F-stars in a 3.15 d orbit with a small eccentricity. Its eclipses were discovered in data from the *Hipparcos* satellite and a spectroscopic orbit was obtained by Griffin^{1,2}. Griffin found a long-term variation of the systemic velocity of the eclipsing system due to a third body in a highly eccentric orbit ($e = 0.73$) with a period of 4200 d. We have used these data, the light curve of V455 Aur from the *TESS* satellite, and the *Gaia* EDR3 parallax to determine the physical properties of the components of the system to high precision. We find the eclipsing stars to have masses of $1.289 \pm 0.006 M_{\odot}$ and $1.232 \pm 0.005 M_{\odot}$, radii of $1.389 \pm 0.011 R_{\odot}$ and $1.318 \pm 0.014 R_{\odot}$ and effective temperatures of 6500 ± 200 and 6400 ± 200 K. Light from the tertiary component is directly detected for the first time, in the form of a third light of $\ell_3 = 0.028 \pm 0.002$ in the solution of the *TESS* light curve. From this ℓ_3 , theoretical spectra and empirical calibrations we estimate the star to have a mass of $0.72 \pm 0.05 M_{\odot}$, a radius of $0.74 \pm 0.05 R_{\odot}$ and a temperature of 4300 ± 300 K. The inclination of the outer orbit is $53 \pm 3^{\circ}$, so the two orbits in the system are not coplanar. We show that a measured spectroscopic light ratio of the two eclipsing stars could lower the uncertainties in radius from 1% to 0.25%. A detailed spectroscopic analysis could also yield precise temperatures and chemical abundances of the system, thus making V455 Aur one of the most precisely measured eclipsing systems known.

Introduction

The study of detached eclipsing binaries (dEBs) is a mature area of research^{3–7} that provides foundational measurements of the physical properties of normal stars against which our theoretical understanding can be compared, verified and improved^{8–12}. Many dEBs have long observational histories, stretching in some cases to over a century^{13,14}. For these objects, and many others, the ongoing NASA Transiting Exoplanet Survey Satellite¹⁵ (*TESS*) mission is providing light curves of previously unobtainable quality. Whilst the *TESS* data are relatively poor in comparison to the NASA *Kepler* satellite¹⁶, they cover a much larger sky area and thus capture information on many more dEBs than *Kepler* did. *TESS* light curves have been used to provide high-quality measurements of the radii of the components of dEBs^{17,18}, discover pulsations in well-known

Table I: *Basic information on V455 Aur*

<i>Property</i>	<i>Value</i>	<i>Reference</i>
Henry Draper designation	HD 45191	34
<i>Hipparcos</i> designation	HIP 30878	35
<i>Tycho</i> designation	TYC 3388-1017-1	36
<i>Gaia</i> EDR3 designation	992435451683384320	37
<i>Gaia</i> EDR3 parallax	12.874 ± 0.052 mas	37
<i>B</i> magnitude	7.71 ± 0.01	36
<i>V</i> magnitude	7.28 ± 0.01	36
<i>J</i> magnitude	6.353 ± 0.019	38
<i>H</i> magnitude	6.132 ± 0.038	38
<i>K_s</i> magnitude	6.082 ± 0.024	38
Spectral type	F5 V + F6 V	This work

dEBs^{19–23}, obtain eclipse timings²⁴, study apsidal motion²⁵, discover multiply-eclipsing binaries^{26,27} and investigate heartbeat stars²⁸.

Within this context we have begun a project to utilise the *TESS* database of time-series photometry to revise and improve the measured physical properties of known dEBs^{29–32}. The principle aim is to curate the Detached Eclipsing Binary Catalogue* (DEBCat) of dEBs with masses and radii measured to precisions of 2% or better³³, by reanalysing existing systems or by adding new dEBs for which good radial velocity (RV) curves already exist.

V455 Aurigae

In this work we present the first measurements of the masses and radii of the components of V455 Aur (Table I). This object was discovered to be eclipsing using *Hipparcos* data³⁵ and given its variable-star designation shortly afterwards³⁹. Fig. 1 shows a plot of the *Hipparcos* epoch photometry.

Griffin¹ presented the first spectroscopic orbit of the system, based on photoelectric observations from the Cambridge *CORAVEL*. A total of 42 RVs were measured for each star. The relatively early spectral type for this instrument proved not to be a problem due to the brightness of the system, although the dips in the cross-correlation functions (CCFs) were only approximately 4% deep (his fig. 4). The resulting spectroscopic orbits provided the first orbital period determination for this system plus measurement of the minimum masses ($M_{A,B} \sin^3 i$ where i is the orbital inclination) to better than 1% precision. Griffin¹ noticed a change in the systemic velocity between the two observing seasons during which he obtained data, and surmised the presence of a third star on a wider orbit. He also suggested that the spectral type of F2 from the Henry Draper Catalogue³⁴ was too early, and that a type of approximately F6 V + F7 V better reflected the properties of the system.

Griffin² revisited the system with additional RV measurements in order to establish the properties of the outer orbit. From 123 RVs of each of the two

*<https://www.astro.keele.ac.uk/jkt/debcats/>

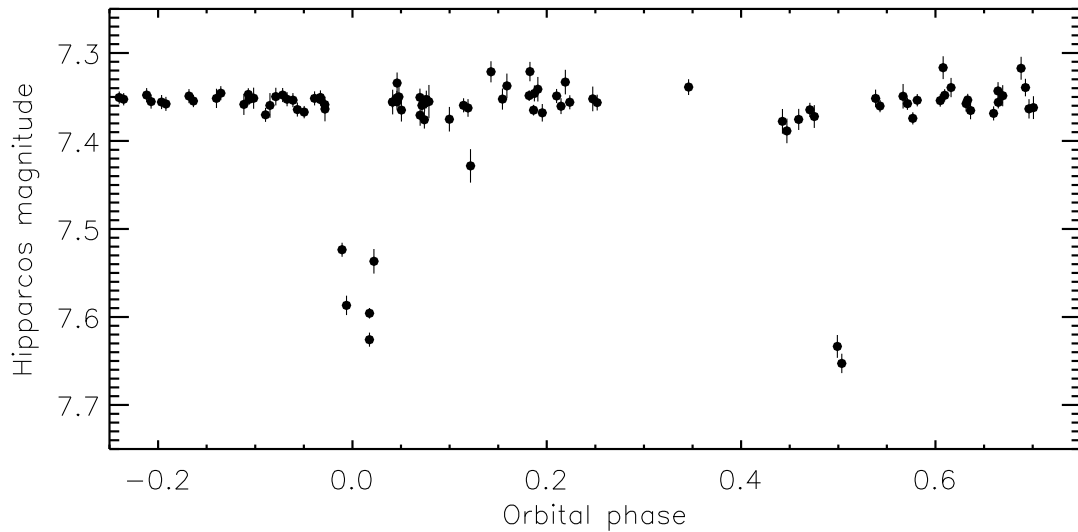


Figure 1: The *Hipparcos* light curve of V455 Aur plotted as a function of orbital phase using the ephemeris determined in the current work.

eclipsing stars he obtained minimum masses to 0.5% precision and confirmed the small but significant orbital eccentricity of the inner orbit. The outer orbit was found to have a period of 4205 ± 17 d, an amplitude of 5.05 ± 0.20 km s⁻¹ and a high eccentricity of 0.726 ± 0.017 . The CCF dips of the two stars have a ratio of 1.21 and this corresponds to a magnitude difference of 0.24 mag in the *V* band; this is of course a measure of the relative strengths of the spectral lines of the two stars, not their continuum brightnesses. The mean projected rotational velocities were found to be 17.98 ± 0.17 km s⁻¹ and 18.77 ± 0.29 km s⁻¹. Griffin² constrained the mass of the tertiary component to be more than $0.5 M_{\odot}$ based on the mass function of the outer orbit, but of spectral type K or later due to the absence of a signal in the CCF.

There are only two other studies that provide relevant information on V455 Aur. Casagrande *et al.*⁴⁰ obtained an effective temperature of $T_{\text{eff}} = 6405 \pm 80$ K and a metallicity of $[\text{Fe}/\text{H}] = -0.25$ for the system using calibrations based on Strömgren photometry. Binarity was not accounted for in the determination of these values, so they should be treated with caution. The T_{eff} listed in the *TESS* Input Catalogue (TIC) version 8.0 (Stassun *et al.*⁴¹) is 6406 ± 142 K. One time of minimum light has been observed by the BAV⁴².

Observational material

The data used in this work comprise a light curve from camera 1 of the NASA *TESS* satellite¹⁵, which observed V455 Aur in Sector 20 (2019/12/24 to 2020/01/21). The light curve covers seven primary and eight secondary eclipses. These data were downloaded from the MAST archive[†] and converted to relative magnitude. We retained only those datapoints with the QUALITY flag equal

[†]Mikulski Archive for Space Telescopes,
<https://mast.stsci.edu/portal/Mashup/Clients/Mast/Portal.html>

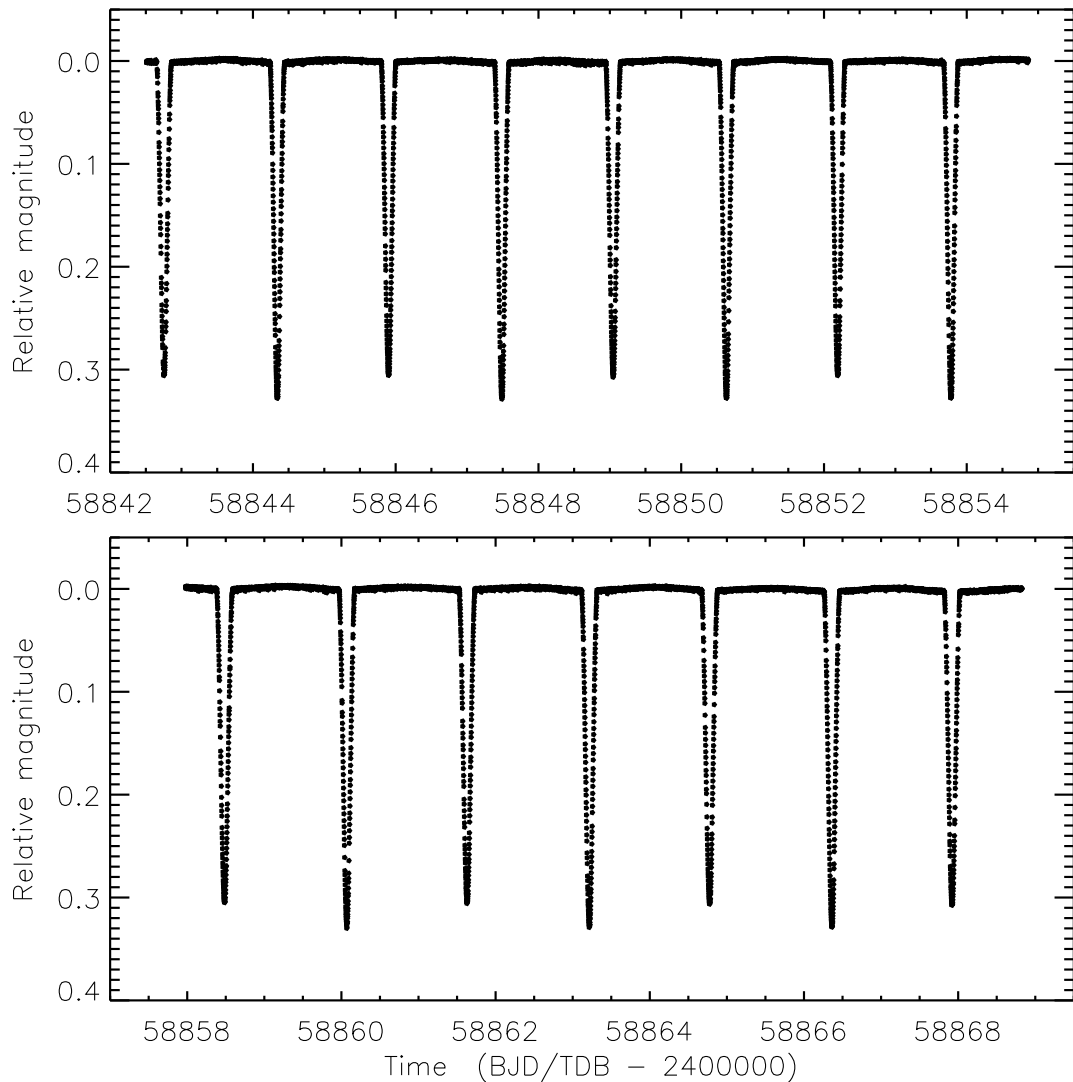


Figure 2: *TESS* Sector 20 short-cadence photometry of V455 Aur. The two panels show the data before and after the mid-sector pause for download of the data to Earth¹⁵.

to zero. The contamination ratio in the TIC v8.0 is 0.011 which indicates very little contaminating light in the *TESS* photometric aperture.

The *TESS* data were obtained in short cadence mode, with a sampling rate of 120 s, and include 16 412 datapoints (Fig. 2). They are available, as usual, in two flavours: simple aperture photometry (SAP) and pre-search data conditioning (PDC)⁴³. As with previous papers in this series, we have chosen to adopt the SAP data for further analysis. This is because the eclipse shapes are indistinguishable between the two datasets but the PDC data contain jumps and slow undulations that have been introduced by the PDC correction process.

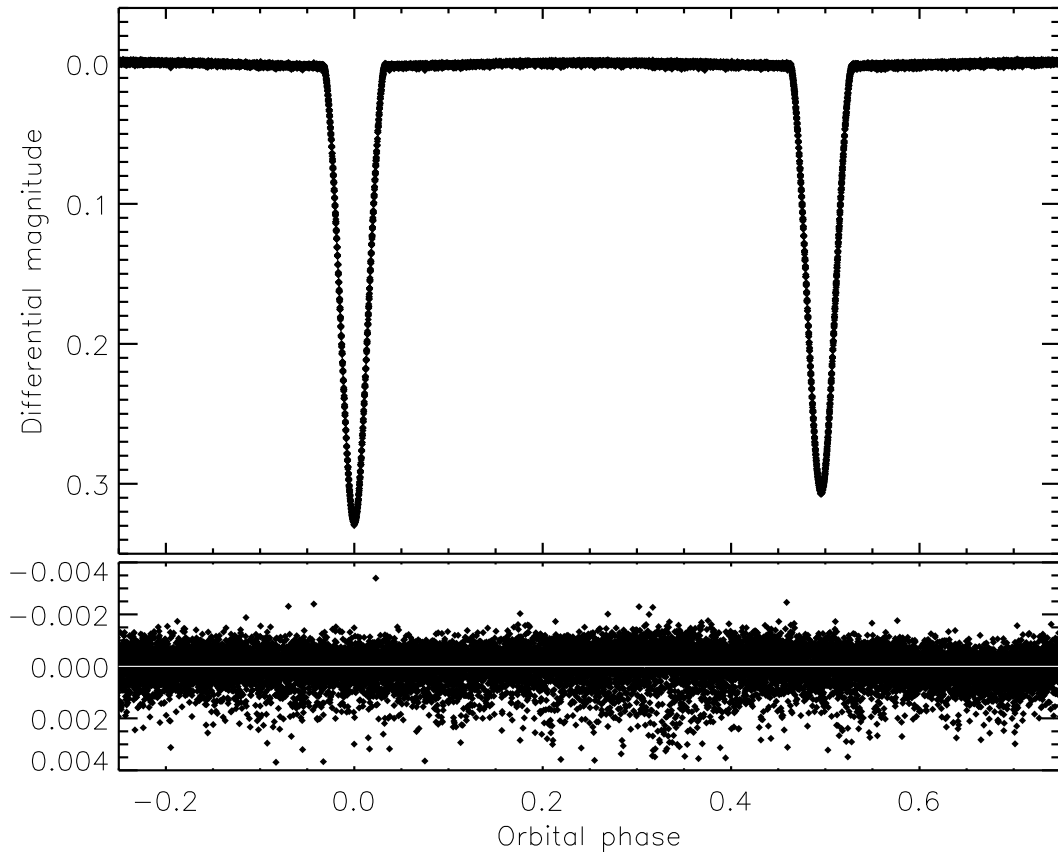


Figure 3: The *TESS* light curve of V455 Aur (filled circles) compared to the JKTEBOP fit (solid line, not visible in front of the data). The lower panels show the residuals of the fit with the line of zero residual overplotted in white for clarity.

Light curve analysis

The components of V455 Aur are small compared to their separation so we adopted version 41 of the JKTEBOP[‡] code^{44,45} for our analysis of the *TESS* light curve. JKTEBOP is fast and flexible, and agrees well with more sophisticated codes when the stars are well-detached¹⁷. We label the star eclipsed at the primary (deeper) eclipse as star A, and its companion as star B; in this case star A is hotter, larger and more massive than star B.

We modelled the *TESS* data and did not consider any additional information such as RVs or times of minimum light. This is because the system has a third body which modifies the observed RVs and times of eclipse of the system, and measuring this change is not a goal of the current work. We fitted for the orbital period and a reference time of primary mid-eclipse. We also fitted for the fractional radii ($r_A = \frac{R_A}{a}$ and $r_B = \frac{R_B}{a}$ where R_A and R_B are the true radii of the stars, and a is the semimajor axis of the relative orbit), parameterised as their sum ($r_A + r_B$) and ratio ($k = \frac{r_B}{r_A}$), the orbital inclination (i) and the central surface brightness ratio (J). As V455 Aur is a triple system we also fitted for the third light (ℓ_3) to account for the contribution of the fainter tertiary component;

[‡]<http://www.astro.keele.ac.uk/jkt/codes/jktebop.html>

Table II: *Parameters of the best JKTEBOP fit to the TESS light curve of V455 Aur. The uncertainties are 1σ . The same limb darkening coefficients were used for both stars.*

<i>Parameter</i>	<i>Value</i>
<i>Fitted parameters:</i>	
Primary eclipse time (BJD/TDB)	$2458853.778650 \pm 0.000008$
Orbital period (d)	3.145777 ± 0.000004
Orbital inclination ($^\circ$)	84.997 ± 0.021
Sum of the fractional radii	0.22018 ± 0.00024
Ratio of the radii	0.949 ± 0.017
Central surface brightness ratio	0.9543 ± 0.0011
Third light	0.0282 ± 0.0022
Linear limb darkening coefficient	0.221 ± 0.012
Quadratic limb darkening coefficient	0.22 (fixed)
$e \cos \omega$	-0.006803 ± 0.000007
$e \sin \omega$	0.00712 ± 0.00037
<i>Derived parameters:</i>	
Fractional radius of star A	0.1130 ± 0.0009
Fractional radius of star B	0.1072 ± 0.0011
Orbital eccentricity	0.00985 ± 0.00027
Argument of periastron ($^\circ$)	133.7 ± 1.5
Light ratio	0.859 ± 0.031

ℓ_3 is defined as the fractional amount of the total light from the system at phase 0.25 that is not contributed by the two eclipsing stars.

The limb darkening was accounted for using the quadratic law⁴⁶, for which we took coefficients from Claret⁴⁷. We fixed the quadratic coefficient to the theoretical value but fitted for the linear coefficient, requiring the coefficients to be the same for both stars due to their similarity in T_{eff} and surface gravity. Fixing one of the two coefficients is acceptable as they are strongly correlated^{48,49} so any imprecision in one coefficient is easily accounted for by a similar change in the other.

A small but highly significant orbital eccentricity (e) was found by Griffin^{1,2} and we find that this is also required in order to get a good fit to the *TESS* data. We accounted for the eccentric orbit by fitting for the parameters $e \cos \omega$ and $e \sin \omega$, where ω is the argument of periastron. Finally, we applied polynomial fits to the overall brightness of the system to deal with any slow changes in brightness, likely of instrumental origin, during the *TESS* observations. We used two first-order polynomials, one for each half of the data (i.e. the two panels in Fig. 2) and fitted the coefficients simultaneously with the other parameters in JKTEBOP.

The best JKTEBOP fit to the *TESS* data is shown in Fig. 3 and is very good. The residuals have a hint of a non-Gaussian distribution to them – they scatter more to fainter than brighter magnitudes – an effect that we have often seen in *TESS* light curves. The parameters of the fit are given in Table II. The secondary eclipse occurs at orbital phase 0.4967.

Determinacy of the photometric parameters

V455 Aur is a system where one might expect to find significant correlations between parameters, as it exhibits partial eclipses and third light. In addition, it has an eccentric orbit and $e \sin \omega$ is often correlated with the ratio of the radii and the orbital inclination. We therefore explored this in detail.

First, we determined the uncertainties in the photometric parameters using three approaches: the Monte Carlo and residual-permutation algorithms in JKTEBOP^{50,49} and by fitting subsections of the light curve in isolation. For the Monte Carlo and residual-permutation algorithms we calculated 10 000 individual solutions. For the fitting-subsections approach we broke the *TESS* data into five sets, each containing three consecutive eclipses, and modelled each in the same way as for the whole dataset. As a result, each fitted and derived parameter had three estimates of its uncertainty, and we simply adopted the largest of the three possibilities (see Table II). All three error estimates were reassuringly similar for all parameters (except the orbital period for obvious reasons), supporting the reliability of the error estimates. The fractional radii are the most important parameters from this analysis and the largest uncertainty estimate for them came from the fitting of subsections of the light curve. They are determined to approximately 1% precision, which is a good result for a partially-eclipsing system with an eccentric orbit and third light.

We find an extremely good agreement with the results from the RV observations by Griffin² for those parameters in common. They comprise the orbital eccentricity (0.0099 ± 0.00012 from Griffin versus 0.0099 ± 0.0003 here), argument of periastron ($132 \pm 7^\circ$ versus $133.7 \pm 1.5^\circ$), and the period (3.1457741 ± 0.0000012 d versus 3.145777 ± 0.000004 d). We also detect the third light to high significance, with a value approximately 13 times its uncertainty, which is the first detection of light from the tertiary component of the system.

To further illustrate the situation we have plotted the results from the Monte Carlo (left panels) and residual-permutation (right panels) algorithms in Fig. 4. An immediate conclusion is that the Monte Carlo algorithm appears to be better-behaved, although this is illusory. The paths traced by various solutions in the residual-permutation panels are a result of correlated noise moving gradually through the light curve, meaning successive residual-permutation solutions are closely related. This does not happen for the Monte Carlo solutions, leading to the smoother appearance of the correlation plots from this algorithm.

Fig. 4 also shows that the sum and ratio of the radii are almost uncorrelated (which is the reason why the fractional radii are parameterised as such in JKTEBOP) but there is a clear correlation between k and $e \sin \omega$. Third light is surprisingly not correlated with the ratio of the radii, but in the case of V455 Aur it is correlated with the orbital inclination and the sum of the fractional radii (not shown).

The primary indeterminacy in the solution is best seen with the ratio of the radii (Fig. 5), which is strongly correlated with the light ratio and thus the surface brightness ratio. Because $r_A + r_B$ is known very precisely from the eclipse durations (its uncertainty in Table II is only 0.1%), k is correlated with r_B and

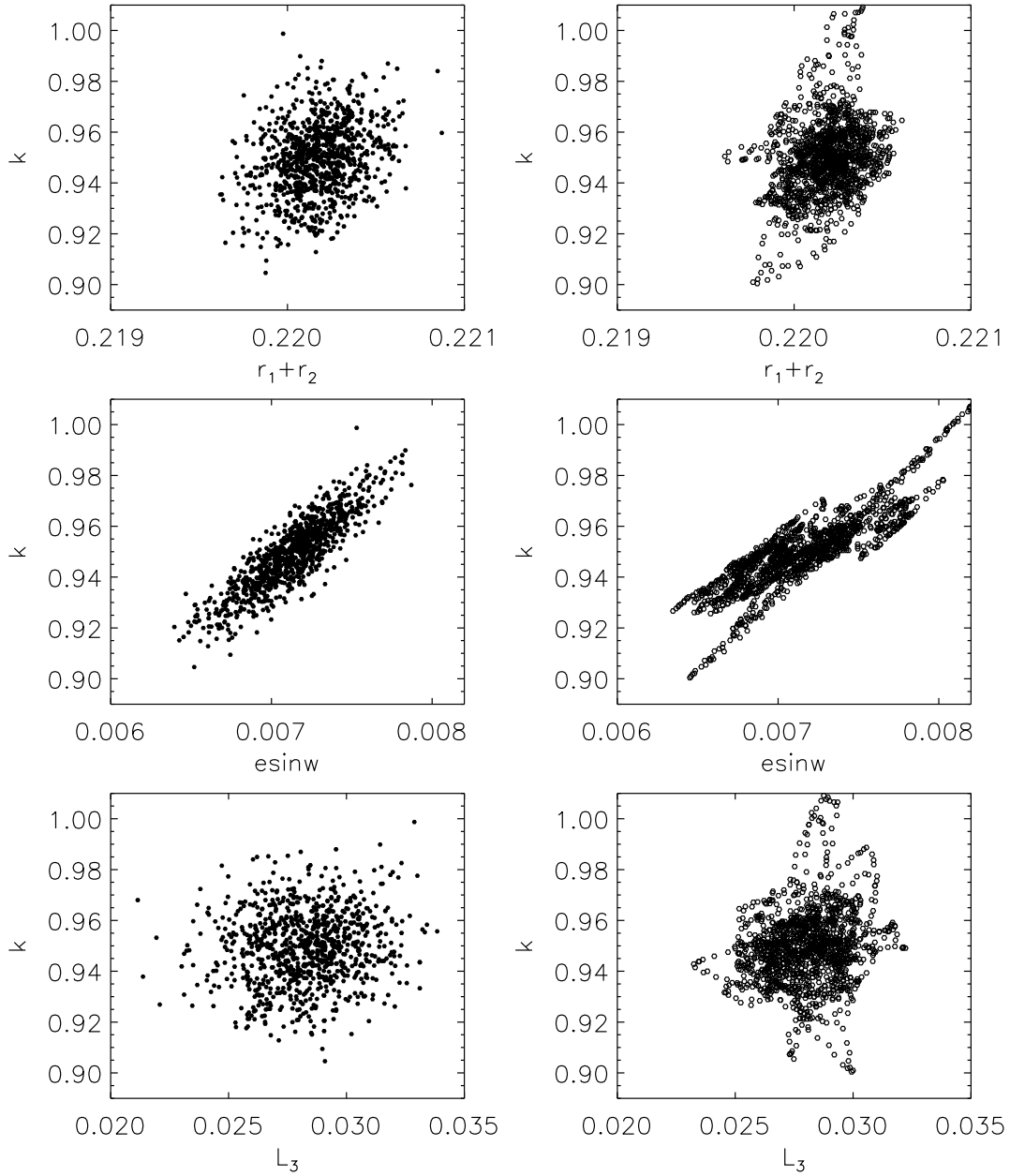


Figure 4: Correlation plots for selected photometric parameters. The panels on the left show results from the Monte Carlo analysis, and on the right from the residual-permutation analysis. Each point corresponds to the best fit of one of the synthetic datasets generated during the error analyses. For clarity, only the first 1000 points are shown in each case.

anti-correlated with r_A .

The net result is that the fractional radii of the stars are correlated with the light ratio, and thus a more precise measurement of r_B and r_A could be obtained if an external constraint on the light ratio of the system were available. We find that if a light ratio with an uncertainty of 5% were available, the precision of the measurements of r_B and r_A would be improved from 0.8% and 1.0%, respectively, to 0.25% for both. Such a constraint could be obtained spectroscopically^{51,48},

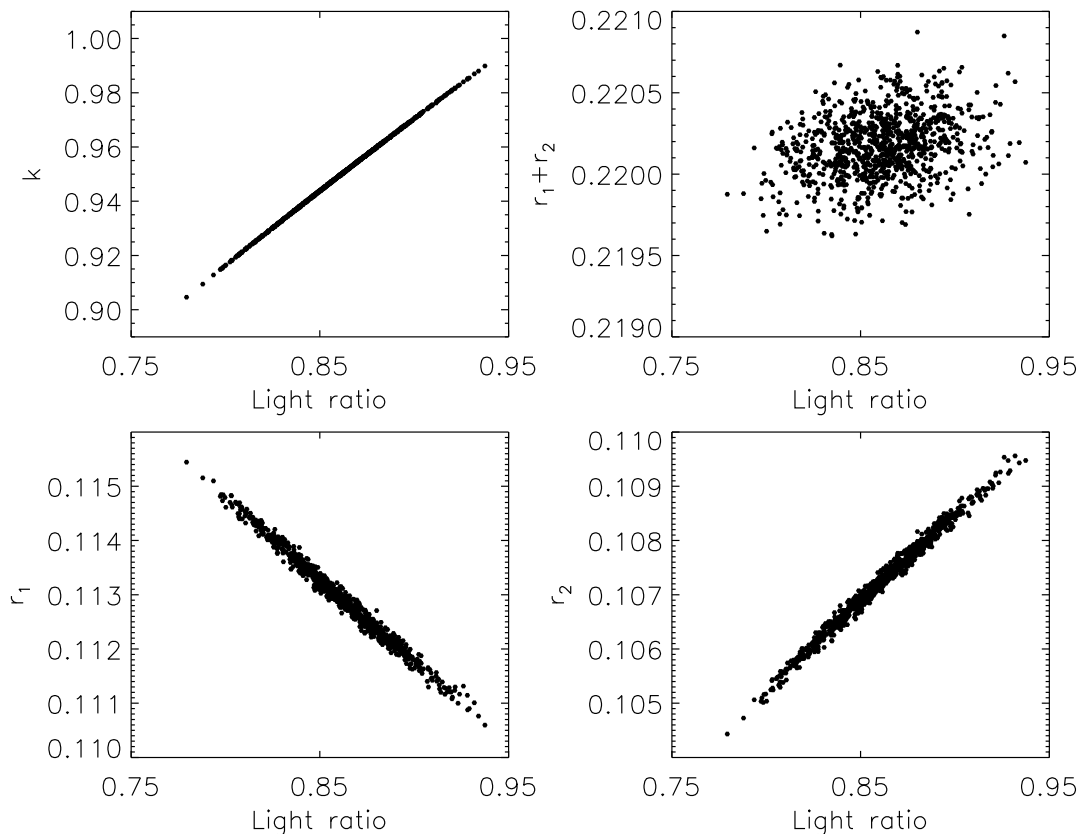


Figure 5: Correlation plots for selected photometric parameters. Each point corresponds to the best fit of a synthetic dataset during the Monte Carlo analysis.

helped by the temperatures of the stars being similar. Another possibility is an interferometric measurement, as achieved for the dEB V1022 Cas^{52,31}. From the physical properties of the system and the *Gaia* EDR3 parallax we find that the angular separation of the stars is 0.735 ± 0.003 mas. This is within the limits of optical interferometers such as CHARA, but difficult and thus less likely to be achieved versus a spectroscopic measurement of the light ratio.

Properties of the third component

Griffin² observed the orbital motion of the tertiary star but not its light. He found that it had to be at least $0.5 M_{\odot}$ in order to cause the observed orbital motion, but of spectral type K or later to remain undetectable in the cross-correlation functions. Now we have a direct measurement of its light – from the third light of $\ell_3 = 0.028 \pm 0.002$ found in the JKTEBOP analysis – it is worth revisiting the topic. This amount of third light is small – especially considering the relatively red response function of *TESS* – so a low-mass third body is expected.

We began by estimating a mass for the tertiary component. The mass was used to predict the radius and T_{eff} of the third body using the empirical polynomial calibrations[§] presented in equations 2 and 3 of Southworth⁵³. Its surface grav-

[§]In Southworth⁵³ calibrations of mass versus radius and mass versus T_{eff} were obtained

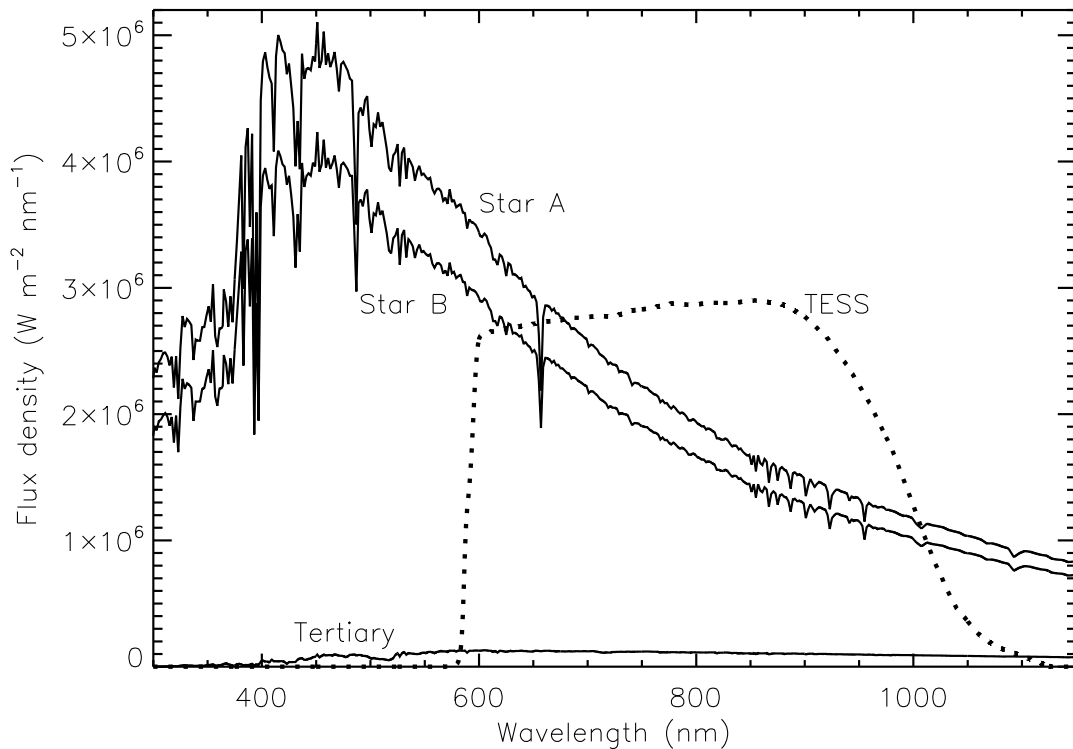


Figure 6: The synthetic spectra of the two eclipsing components (labelled Star A and Star B) and of the third body (labelled Tertiary) from ATLAS9 model atmospheres and adjusted for the radii of the stars. The passband response function from *TESS* is also shown, using dotted lines, and has been arbitrarily scaled to half the full height of the plot.

ity was calculated from its mass and radius. We then interpolated the ATLAS9 synthetic spectra from Castelli *et al.*⁵⁴ to the T_{eff} and gravity values of the star.

The T_{eff} values of the eclipsing stars were initially taken to be 6340 K and 6240 K based on the spectral types advanced by Griffin² and the tables of Pecaut & Mamajek⁵⁵. These values were subsequently revised to 6500 K and 6400 K in a second iteration. Synthetic ATLAS9 spectra were interpolated as for the third star, using their surface gravities from Table III. The three sets of synthetic fluxes were converted to relative light contributions using the radii of the three stars, and then passed through the response function of the *TESS* instrument¹⁵. The third light value was calculated as the fraction of the combined light of the three stars that is emitted by the third star.

We then adjusted the estimated mass of the tertiary component until the predicted amount of third light matched the ℓ_3 measured from the light curve. In the following section we use the properties of the third star in the process of determining the T_{eff} values of the two eclipsing stars. Once this was completed, we reran the analysis above with the new T_{eff} values in order to arrive at consistent values for the properties of the tertiary component.

We found that the tertiary star has a mass of $0.72 \pm 0.05 M_{\odot}$, a radius of $0.74 \pm$

from stars of masses $0.21 M_{\odot}$ to $1.59 M_{\odot}$. The first calibration was used but the second calibration was not; it was retained in that publication in case it became useful in future.

Table III: *Physical properties of V455 Aur defined using the nominal solar units given by IAU 2015 Resolution B3 (Ref. ⁶¹).*

<i>Parameter</i>	<i>Star A</i>	<i>Star B</i>
Mass ratio	0.9557 ± 0.0027	
Semimajor axis of relative orbit (\mathcal{R}_{\odot}^N)	12.295 ± 0.017	
Mass (\mathcal{M}_{\odot}^N)	1.2887 ± 0.0063	1.2316 ± 0.0050
Radius (\mathcal{R}_{\odot}^N)	1.389 ± 0.011	1.318 ± 0.014
Surface gravity (log[cgs])	4.2626 ± 0.0070	4.2887 ± 0.0089
Density (ρ_{\odot})	0.480 ± 0.012	0.538 ± 0.017
Synchronous rotational velocity (km s ⁻¹)	22.38 ± 0.18	21.20 ± 0.22
Effective temperature (K)	6500 ± 200	6400 ± 200
Luminosity log(L/\mathcal{L}_{\odot}^N)	0.492 ± 0.054	0.419 ± 0.055
M_{bol} (mag)	3.51 ± 0.13	3.69 ± 0.14

0.05 R_{\odot} and a T_{eff} of 4300 ± 300 K, where the errorbars include contributions from the third light and also the scatter in the empirical calibrations. The numbers quoted here are those obtained after the iteration to the final T_{eff} values of the two eclipsing stars (see below). A representative plot of the theoretical spectra and the *TESS* passband is shown in Fig. 6. With this mass the inclination of the third orbit is $53 \pm 3^{\circ}$ which implies this triple system is not coplanar.

Using Kepler’s third law we find the semimajor axis of the outer (relative) orbit to be 7.6 au and thus the maximum separation between the eclipsing and the tertiary components is $r_{\text{max}} = a(1 + e) = 13.0$ au. At a distance of 78 pc (see below) this corresponds to an angular separation of $0.17''$. This is resolvable using high-resolution imaging or integral-field spectroscopy of the type often wielded in the detection of close binaries and young planets^{56–58}. Obtaining the spectrum of the third star, or its apparent magnitudes in multiple passbands, would provide additional constraints on its T_{eff} and thus mass. This will be easier at infrared wavelengths due to the brightness of the third component relative to stars A and B: we find that the value of ℓ_3 is only 0.015 in the *V*-band but increases to 0.082 in the *K_s*-band.

Physical properties of the eclipsing system

We used the JKTABSDIM code⁵⁹ to calculate the physical properties of the eclipsing system and its two components. As input to this we used the fractional radii, orbital period, inclination and eccentricity from the photometric analysis above. To this we added the velocity amplitudes measured by Griffin², $K_A = 96.27 \pm 0.16$ km s⁻¹ and $K_B = 100.73 \pm 0.23$ km s⁻¹, on the grounds that there was no clear reason to repeat his analysis rather than just adopt his results. We confirmed that the RVs were correctly attributed to the two stars, as it is possible that the photometric primary star (the star obscured at the deeper eclipse) is not the spectroscopic primary star (the star which is brighter or has stronger spectral lines); for examples see Paper IV of this series³² and Themeßl *et al.*⁶⁰. The masses and radii of the stars obtained in this way are measured to precisions of 0.5% and 1.0%, respectively, which can be attributed to the quality

of the RVs from Griffin² and the light curve from *TESS*.

The remaining quantities to be determined are the T_{eff} values of the three stars detectable in the light curve. This can be done by matching the distance from the *Gaia* EDR3³⁷ parallax, 77.68 ± 0.31 pc, to that obtained from the radii, T_{eff} values and bolometric corrections of the stars. For this we used the bolometric corrections in multiple passbands from Girardi *et al.*⁶². We accounted for interstellar reddening of the system by including an estimate of $E(B - V) = 0.002 \pm 0.002$ mag obtained using the STILISM[¶] online tool (Lallement *et al.*^{63,64}).

The *BV* and *JHK* apparent magnitudes of V455 Aur, given in Table I, include the light from all three components but we have the relative light contributions in only the *TESS* passband. We therefore used estimates of the T_{eff} values of the three components and propagated their relative light contributions in the *TESS* band to the other bands^{65,66} using ATLAS9 synthetic spectra⁵⁴. The T_{eff} ratio of the two eclipsing stars is tightly constrained by the surface brightness ratio from the JKTEBOP analysis. This process was iterated once in order to ensure consistent properties for all three stars (see previous section). Additional iterations were not needed because the third body contributes only a small amount of light to the system. Once these relative light contributions were determined, we calculated the apparent magnitudes and distance of the eclipsing system. By requiring the distances to be consistent in different passbands and with that from the *Gaia* EDR3 parallax, we determined the T_{eff} values of the eclipsing stars by iterative manual adjustment.

We find the T_{eff} values of the two stars to be $T_{\text{eff,A}} = 6500 \pm 200$ K and $T_{\text{eff,B}} = 6400 \pm 200$ K. These correspond to spectral types of F5 V and F6 V, respectively⁵⁵, which is closer to the F6 V + F7 V favoured by Griffin² than the F2 in the *Henry Draper Catalogue*³⁴. A detailed spectroscopic analysis to determine precise T_{eff} values and chemical abundances would be very beneficial in improving our understanding of this system^{67,68}.

Summary

The V455 Aur system comprises a double-lined spectroscopic binary with a lower-mass third star on a wider orbit. The inner binary was found to be eclipsing from its *Hipparcos* light curve. Extensive RV measurements by Griffin^{1,2} yielded precise measurements of the masses of the two eclipsing stars and the first determination of the period of the outer orbit. Prior to the current analysis, however, no photometric study of the system was available.

In this work we have studied the high-quality light curve of V455 Aur obtained by the *TESS* satellite, which covers seven orbital periods of the inner eclipsing system. We determined precise fractional radii for the two stars and also detected the light contribution of the third star to high confidence. Combining our photometric results with the spectroscopic quantities from Griffin², we have determined the masses and radii of the eclipsing stars to precisions of 0.5% and 1.0%, respectively. We have shown that the radius measurements could be further improved by obtaining a spectroscopic light ratio.

¶<https://stilism.obspm.fr>

The T_{eff} values of the dEB were measured by forcing the distance to the system (determined from the stellar radii and T_{eff} values) to match that found from the *Gaia* EDR3 parallax. As part of this process we subtracted the contribution of the third star from the apparent magnitudes of the system in the *BV* and *JHK* bands, and accounted for interstellar extinction using reddening maps^{63,64}. The mass, radius and T_{eff} of the tertiary was obtained from empirical calibrations based on dEBs⁵³ adjusted to match its light contribution to the *TESS* light curve. Its mass is significantly above the minimum mass from the outer spectroscopic orbit, suggesting that the two orbits are not coplanar.

We have made a brief comparison of the properties of V455 Aur AB to the predictions of the PARSEC theoretical stellar models⁶⁹. We find that the masses, radii and T_{eff} values are reasonably well matched for a fractional metal abundance of $Z = 0.017 \pm 0.003$ and an age of 1.8 ± 0.2 Gyr. The model predictions are slightly too shallow to match the observed mass–radius relation of the two stars, with an agreement at the level of roughly 2σ . This should be investigated in more detail in future, once further constraints have been placed on the physical properties of V455 Aur.

With these new results V455 Aur can be added to the DEBCat catalogue³³. A detailed spectroscopic analysis of the system is advocated, in order to provide better T_{eff} measurements of the stars as well as a light ratio (helpful in measuring their radii) and photospheric chemical abundances (useful for a comparison with theoretical models). The complication caused by the presence of the third body means this is not a benchmark binary system, as the third light affects the photometric analysis, but the non-coplanarity of the two orbits is interesting from a dynamical viewpoint⁷⁰.

Acknowledgements

The current work presented a detailed analysis of an eclipsing binary system that was only made possible by the extensive and impressive RV dataset obtained by Roger Griffin. This work was begun shortly before Roger passed away at the age of 85. I wish to dedicate this paper to Roger, who provided an extraordinary example of what can be achieved via careful analysis of many objects as part of a long-term project. Whilst I never met Roger, I have had the privilege of several lengthy email exchanges with him as well as a brief tour of “his” 36-inch telescope at Cambridge.

I thank Kresimir Pavlovski and Dariusz Graczyk for comments on a draft of this manuscript. This paper includes data collected by the *TESS* mission. Funding for the *TESS* mission is provided by the NASA’s Science Mission Directorate. The following resources were used in the course of this work: the NASA Astrophysics Data System; the SIMBAD database operated at CDS, Strasbourg, France; and the arXiv scientific paper preprint service operated by Cornell University.

References

- (1) R. F. Griffin, *The Observatory*, **121**, 315, 2001.

- (2) R. F. Griffin, *The Observatory*, **133**, 156, 2013.
- (3) H. N. Russell, *Nature*, **93**, 252, 1914.
- (4) D. M. Popper, *ARA&A*, **5**, 85, 1967.
- (5) D. M. Popper, *ARA&A*, **18**, 115, 1980.
- (6) J. Andersen, *A&ARv*, **3**, 91, 1991.
- (7) G. Torres, J. Andersen & A. Giménez, *A&ARv*, **18**, 67, 2010.
- (8) J. Andersen, J. V. Clausen & B. Nordström, *ApJL*, **363**, L33, 1990.
- (9) O. R. Pols *et al.*, *MNRAS*, **289**, 869, 1997.
- (10) F. Spada *et al.*, *ApJ*, **776**, 87, 2013.
- (11) A. Claret & G. Torres, *ApJ*, **859**, 100, 2018.
- (12) A. Tkachenko *et al.*, *A&A*, **637**, A60, 2020.
- (13) J. Stebbins, *ApJ*, **34**, 112, 1911.
- (14) J. Stebbins, *ApJ*, **54**, 81, 1921.
- (15) G. R. Ricker *et al.*, *Journal of Astronomical Telescopes, Instruments, and Systems*, **1**, 014003, 2015.
- (16) W. J. Borucki, *Reports on Progress in Physics*, **79**, 036901, 2016.
- (17) P. F. L. Maxted *et al.*, *MNRAS*, **498**, 332, 2020.
- (18) D. Graczyk *et al.*, *A&A*, *in press*, [arXiv:2103.02077](https://arxiv.org/abs/2103.02077), 2021.
- (19) J. Southworth *et al.*, *MNRAS*, **497**, L19, 2020.
- (20) J. W. Lee & K. Hong, *AJ*, **161**, 32, 2021.
- (21) J. Southworth, D. M. Bowman & K. Pavlovski, *MNRAS*, **501**, L65, 2021.
- (22) E. Budding *et al.*, *MNRAS*, *in press*, [arXiv:2102.00362](https://arxiv.org/abs/2102.00362), 2021.
- (23) J. W. Lee, K. Hong & H.-Y. Kim, *AJ*, **161**, 129, 2021.
- (24) C. von Essen *et al.*, *AJ*, *in press*, [arXiv:2005.07203](https://arxiv.org/abs/2005.07203), 2020.
- (25) D. Baroch *et al.*, *A&A*, *in press*, [arXiv:2103.03140](https://arxiv.org/abs/2103.03140), 2021.
- (26) T. Borkovits *et al.*, *MNRAS*, **496**, 4624, 2020.
- (27) T. Borkovits *et al.*, *MNRAS*, *in press*, [arXiv:2103.00925](https://arxiv.org/abs/2103.00925), 2021.
- (28) P. A. Kołaczek-Szymański *et al.*, *A&A*, **647**, A12, 2021.
- (29) J. Southworth, *The Observatory*, **140**, 247, 2020.
- (30) J. Southworth, *The Observatory*, **141**, 22, 2021.
- (31) J. Southworth, *The Observatory*, **141**, 52, 2021.
- (32) J. Southworth, *The Observatory*, *in press*, [arXiv:2103.03644](https://arxiv.org/abs/2103.03644), 2021.
- (33) J. Southworth, in *Living Together: Planets, Host Stars and Binaries* (S. M. Rucinski, G. Torres & M. Zejda, eds.), 2015, *Astronomical Society of the Pacific Conference Series*, vol. 496, p. 321.
- (34) A. J. Cannon & E. C. Pickering, *Annals of Harvard College Observatory*, **92**, 1, 1918.
- (35) ESA (ed.), *The HIPPARCOS and TYCHO catalogues. Astrometric and photometric star catalogues derived from the ESA HIPPARCOS Space Astrometry Mission*, *ESA Special Publication*, vol. 1200, 1997.
- (36) E. Høg *et al.*, *A&A*, **355**, L27, 2000.
- (37) Gaia Collaboration *et al.*, *A&A*, *in prep*, [arXiv:2012.01533](https://arxiv.org/abs/2012.01533), 2020.
- (38) R. M. Cutri *et al.*, *2MASS All Sky Catalogue of Point Sources* (The IRSA 2MASS All-Sky Point Source Catalogue, NASA/IPAC Infrared Science Archive, Caltech, US), 2003.
- (39) E. V. Kazarovets *et al.*, *Information Bulletin on Variable Stars*, **4659**, 1, 1999.
- (40) L. Casagrande *et al.*, *A&A*, **530**, A138, 2011.
- (41) K. G. Stassun *et al.*, *AJ*, **158**, 138, 2019.
- (42) J. Hubscher, *IBVS*, **6152**, 1, 2015.
- (43) J. M. Jenkins *et al.*, in *Proc. SPIE*, 2016, *Society of Photo-Optical Instrumentation Engineers (SPIE) Conference Series*, vol. 9913, p. 99133E.
- (44) J. Southworth, P. F. L. Maxted & B. Smalley, *MNRAS*, **351**, 1277, 2004.
- (45) J. Southworth, *A&A*, **557**, A119, 2013.
- (46) Z. Kopal, *Harvard College Observatory Circular*, **454**, 1, 1950.

- (47) A. Claret, *A&A*, **618**, A20, 2018.
- (48) J. Southworth, H. Bruntt & D. L. Buzasi, *A&A*, **467**, 1215, 2007.
- (49) J. Southworth, *MNRAS*, **386**, 1644, 2008.
- (50) J. Southworth, P. F. L. Maxted & B. Smalley, *MNRAS*, **349**, 547, 2004.
- (51) G. Torres *et al.*, *AJ*, **120**, 3226, 2000.
- (52) K. V. Lester *et al.*, *AJ*, **157**, 140, 2019.
- (53) J. Southworth, *MNRAS*, **394**, 272, 2009.
- (54) F. Castelli, R. G. Gratton & R. L. Kurucz, *A&A*, **318**, 841, 1997.
- (55) M. J. Pecaut & E. E. Mamajek, *ApJS*, **208**, 9, 2013.
- (56) D. F. Evans, J. Southworth & B. Smalley, *ApJ*, **833**, L19, 2016.
- (57) J. L. Beuzit *et al.*, *A&A*, **631**, A155, 2019.
- (58) B. Macintosh *et al.*, *PNAS*, **111**, 12661, 2014.
- (59) J. Southworth, P. F. L. Maxted & B. Smalley, *A&A*, **429**, 645, 2005.
- (60) N. Themeßl *et al.*, *MNRAS*, **478**, 4669, 2018.
- (61) A. Prša *et al.*, *AJ*, **152**, 41, 2016.
- (62) L. Girardi *et al.*, *A&A*, **391**, 195, 2002.
- (63) R. Lallement *et al.*, *A&A*, **561**, A91, 2014.
- (64) R. Lallement *et al.*, *A&A*, **616**, A132, 2018.
- (65) J. Southworth *et al.*, *MNRAS*, **408**, 1680, 2010.
- (66) J. Southworth *et al.*, *A&A*, **635**, A74, 2020.
- (67) K. Pavlovski *et al.*, *MNRAS*, **438**, 590, 2014.
- (68) G. Torres *et al.*, *ApJ*, **797**, 31, 2014.
- (69) A. Bressan *et al.*, *MNRAS*, **427**, 127, 2012.
- (70) A. Tokovinin, *ApJS*, **235**, 6, 2018.